

Characterization of zero-bias microwave diode power detectors at cryogenic temperature

Vincent Giordano, Christophe Fluhr, Benoît Dubois, and Enrico Rubiola

Citation: [Review of Scientific Instruments](#) **87**, 084702 (2016); doi: 10.1063/1.4960087

View online: <http://dx.doi.org/10.1063/1.4960087>

View Table of Contents: <http://scitation.aip.org/content/aip/journal/rsi/87/8?ver=pdfcov>

Published by the [AIP Publishing](#)

Articles you may be interested in

[Performance evaluation of a lossy transmission lines based diode detector at cryogenic temperature](#)
Rev. Sci. Instrum. **87**, 014706 (2016); 10.1063/1.4939730

[Modeling of microwave diode on diamond like coating Si cathode](#)
J. Vac. Sci. Technol. B **33**, 03C110 (2015); 10.1116/1.4906821

[Graphene self-switching diodes as zero-bias microwave detectors](#)
Appl. Phys. Lett. **106**, 093116 (2015); 10.1063/1.4914356

[Experimental characterization and modeling of the bending strain effect on flexible microwave diodes and switches on plastic substrate](#)
Appl. Phys. Lett. **99**, 243104 (2011); 10.1063/1.3668112

[Temperature investigation of dark current and its electrical noise in GaAs/AlGaAs multi-quantum well photodiodes](#)
J. Appl. Phys. **85**, 1211 (1999); 10.1063/1.369343



Characterization of zero-bias microwave diode power detectors at cryogenic temperature

Vincent Giordano,^{1,a)} Christophe Fluhr,¹ Benoît Dubois,² and Enrico Rubiola^{1,b)}

¹*Time and Frequency Department, CNRS FEMTO-ST Institute (UMR 6174), 26 Chemin de l'Épitaphe, 25030 Besançon, France*

²*FEMTO Engineering, 32 Avenue de l'Observatoire 25000 Besançon, France*

(Received 5 April 2016; accepted 19 July 2016; published online 23 August 2016)

We present the characterization of commercial tunnel diode low-level microwave power detectors at room and cryogenic temperatures. The sensitivity as well as the output voltage noise of the tunnel diodes is measured as functions of the applied microwave power. We highlight strong variations of the diode characteristics when the applied microwave power is higher than a few microwatts. For a diode operating at 4 K, the differential gain increases from 1000 V/W to about 4500 V/W when the power passes from -30 dBm to -20 dBm. The diode white noise floor is equivalent to a Noise Equivalent Power of 0.8 pW/ $\sqrt{\text{Hz}}$ and 8 pW/ $\sqrt{\text{Hz}}$ at 4 K and 300 K, respectively. Its flicker noise is equivalent to a relative amplitude noise power spectral density $S_{\alpha}(1 \text{ Hz}) = -120$ dB/Hz at 4 K. Flicker noise is 10 dB higher at room temperature. *Published by AIP Publishing.* [<http://dx.doi.org/10.1063/1.4960087>]

I. INTRODUCTION

Tunnel diodes are known to be very efficient low-level microwave power detectors. They are available off-the-shelf from numerous manufacturers in the form of small packaged coaxial components that can be easily implemented in any microwave system. They are used in power, Amplitude Modulation (AM) noise measurement, control, and monitoring systems. Tunnel detectors are actually backward detectors. The backward diode is a tunnel diode in which the negative resistance in the forward-bias region is made negligible by appropriate doping and used in the reverse-bias region. Most of the work on such detectors dates back to the sixties.¹⁻³ Tunnel detectors exhibit fast switching and higher gain than the Schottky counterpart. Tunnel diodes also work in a cryogenic environment, provided the package tolerates the mechanical stress of the thermal contraction. Looking at the specifications of commercial power detectors, information about noise is scarce. Some manufacturers give the NEP (Noise Equivalent Power) parameter, i.e., the power at the detector input that produces a video output equal to that of the device noise. In no case is it said whether the NEP increases or not in the presence of a strong input signal, which is related to precision. Even worse, no data about flickering are found in the literature or in the data sheets.

In this paper we present a characterization of commercial tunnel diodes (Model Herotek DT8012). Such diodes are implemented in our 10 GHz ultra-stable Cryogenic Sapphire Oscillators (CSOs).^{4,5} The CSO is currently the most stable microwave source achieving better than 1×10^{-15} fractional frequency stability at short term.⁶ The CSO is a Pound-Galani oscillator.⁷ In short, the resonator is used in transmission

mode in a regular oscillator loop and in reflection mode as the discriminator of the classical Pound servo.⁸ The CSO frequency is affected by the power fluctuation of the microwave signal incident on the sapphire resonator.^{9,10} A power control needs to be implemented to reach the best possible frequency stability. Two tunnel diodes are used as low-level detectors to detect the small changes in the phase and the power of the signal in the oscillating loop. In this way they are key components as their sensitivity conditions the CSO frequency stability. In this application the measurement bandwidth is limited to 100 kHz, and we thus do not explore the switching capability of the tunnel diode and restrict our characterisation to the low frequency sensitivity.

First, we introduce the topic of AM noise measurement. The tested diodes' specifications and the corresponding electrical model are given in Section III. Then we describe the experimental set-up and the power-to-voltage gain measurements (Section IV). The principle and the results of the diode intrinsic noise measurements are presented in Section V.

II. AM NOISE MEASUREMENT BASICS

Our diode detectors are intended to measure the small power fluctuations affecting the signal of an ultra-stable oscillator. Considering only AM noise the RF voltage is

$$V_{RF}(t) = V_0 [1 + \alpha(t)] \cos(2\pi\nu_0 t), \quad (1)$$

where V_0 is the RF voltage mean amplitude, ν_0 is the signal frequency, and $\alpha(t)$ is the fractional amplitude fluctuation. In low noise conditions, we have $|\alpha(t)| \ll 1$ and the instantaneous signal power is

$$P(t) = P_0 + \delta P(t) \approx \frac{V_0^2}{2R_0} (1 + 2\alpha(t)), \quad (2)$$

where $R_0 = 50 \Omega$, and P_0 is the mean signal power. The amplitude fluctuations are measured through the measurement

^{a)}Author to whom correspondence should be addressed. Electronic mail: vincent.giordano@femto-st.fr

^{b)}URL: <http://rubiola.org>.

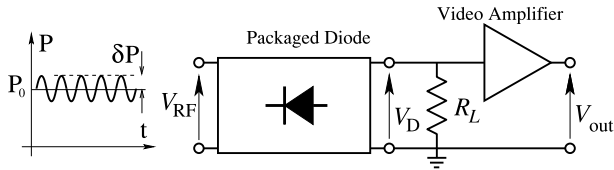


FIG. 1. The basic implementation of a zero-bias microwave power detector.

of the power fluctuation $\delta P(t)$,

$$\alpha(t) = \frac{1}{2} \frac{\delta P(t)}{P_0}, \quad (3)$$

and of its Power Spectrum Density (PSD),

$$S_\alpha(f) = \frac{1}{4} S_{\delta P}(f) = \frac{1}{4P_0^2} S_{\delta P}(f). \quad (4)$$

The basic implementation of a zero-bias microwave power detector is represented in Fig. 1.

The RF voltage is applied to the diode input terminal. The video output is loaded by the video amplifier input impedance R_L . A perfect square-law detector will produce a voltage proportional to P ,

$$V_D(P) = K_D P. \quad (5)$$

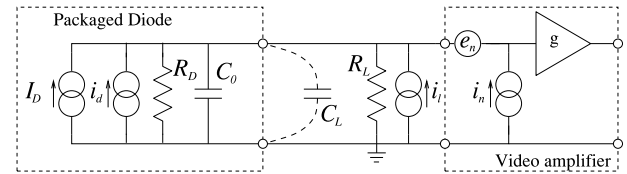
K_D is the detector power-to-voltage gain expressed in V/W, also called *sensitivity* in most of the data-sheets. Manufacturers generally specify K_D measured at room temperature and for an input signal power of -20 dBm or so. Typically for an X-band diode, $K_D \approx 1000$ V/W.

It is generally admitted that Equation (5) holds for a signal power below -20 dBm and then the detector response turns smoothly from quadratic to linear. At high signal power, typically above 0 dBm, the diode is acting as a peak detector. This traditionally accepted view of the diode detector leads to expect a sensitivity K_D almost constant below -20 dBm and then saturating smoothly when the signal power is increased like in Ref. 11. As we will see in the following this simple model is not sufficient to describe the diode behavior on its whole dynamic range. In most cases, the diode output voltage should be written as a non-linear function $\kappa_D(P)$ of the input power. In radiometric measurements the detector transfer function should be known in its whole dynamic range. Various methods are used to account for the nonlinear detector response.¹⁶⁻¹⁸ In the case of AM noise measurement or control, we are only interested in small power fluctuations δP around the mean value P_0 , with $\delta P \ll P_0$. Keeping only the first order term in the Taylor development of the function $\kappa_D(P)$,

$$V_D(P) = \kappa_D(P_0) + \frac{d\kappa_D}{dP}(P_0)\delta P + O(\delta P^2). \quad (6)$$

The diode sensitivity, i.e., the slope of the voltage-to-power curve, should be measured at the actual input power P_0 as it can vary in a large proportion in the whole dynamic range.

Providing that the diode sensitivity is known, $S_\alpha(f)$ is easily determined through the measurement of the detector output voltage PSD. In the absence of power fluctuations, the output voltage V_D is affected by the internal diode noise sources and by the input noise of the video amplifier. This

FIG. 2. Electrical model for the detector video output. The capacitance C_L will be temporarily added to evaluate the differential resistance R_D (see Section IV C).

intrinsic detector noise sets the noise floor of the detection system and needs to be characterized.

III. DIODE SPECIFICATIONS AND ELECTRICAL MODEL

A simplified electrical model for the video part of the power detector is given in Fig. 2.²

R_D is the differential resistance associated with the diode junction. C_0 is the output capacitance required to filter out the RF carrier and harmonics. Here we neglect parasitic resistances and capacitances associated with the bulk semiconductor or connections. They will not change the overall behavior of the diode and can be easily added in a second step if needed. Furthermore we do not seek to deeply understand the physics of the semiconductor but rather to qualify the diode as a low-level power detector. We tested two tunnel diode detectors from Herotek. The diode basic characteristics extracted from the manufacturer data-sheet are given in Table I.

The RF voltage applied to the diode junction is rectified by the non-linear current-voltage characteristic of the device. Dropping the ac-components filtered by C_0 , the rectification process is modeled by the low-frequency current generator I_D . The current I_D is a non-linear function of the RF power.

The intrinsic fluctuations of the diode current are accounted for by the current noise source i_d . For an ideal detector, owing to the shot effect, the average current I_D flowing in the diode junction is affected by a fluctuation of power spectral density

$$S_{i_d}^{shot}(f) = 2qI_D. \quad (7)$$

For $P_0 = -20$ dBm, the diode voltage on a high-load impedance will be $V_D \approx K_D P_0 = 8$ mV and the diode current $I_D = V_D/R_D \approx 64$ μ A. The shot noise is characterized by a noise current density such as $i_d^{shot} = \sqrt{2qI_D} \approx 5$ pA/ $\sqrt{\text{Hz}}$.

TABLE I. Tested tunnel diode specifications. (at 25 °C and for 10 μ W power input).

Model	HEROTEK DT8012
Serial number	SN436409 and SN436410
Frequency range	8–12 GHz
Minimum sensitivity K_D	800 V/W
Typical VSWR	2.5:1
Typical output capacitance C_0	10 pF
Typical differential resistance R_D	125 Ω

The load resistance R_L is associated with the thermal current noise source i_t with a PSD given by

$$S_{i_t(f)} = \frac{4k_B T}{R_L}, \tag{8}$$

where k_B is the Boltzmann constant and T the temperature of the load resistance.

The amplifier voltage and current fluctuations are accounted for by e_n and i_n , according to the popular Rothe-Dahlke model.¹² Our custom video amplifier has 36 dB gain. It is based on an AD743 Junction Field Effect Transistor (JFET) operational amplifier characterized by a very low current noise: $i_n = 7 \text{ fA}/\sqrt{\text{Hz}}$. The voltage noise has been measured with a $50 \text{ }\Omega$ resistance at the amplifier input. The white voltage noise is $e_n = 5 \text{ nV}/\sqrt{\text{Hz}}$. All measurements presented here have been realized with a high load resistance, i.e., $R_L = 1 \text{ M}\Omega$: thus $R_L \gg R_D$. Assuming a noise free incoming RF signal and a shot noise limited detector, the PSD of the voltage fluctuations at the input of the video amplifier will be

$$S_{\delta V_D}(f) = S_{e_n}(f) + R_D^2 [S_{i_d}^{shot}(f) + S_{i_t}(f) + S_{i_n}(f)]. \tag{9}$$

For the simple measurement set-up depicted in Fig. 1 as $R_D \approx 125 \text{ }\Omega$, the contributions of the current noise sources are negligible. The detected noise is mainly limited by the video-amplifier input voltage noise source. For $P_0 = -20 \text{ dBm}$ and $K_D = 800$, the white noise floor is

$$S_{\alpha}(f) = \frac{S_{e_n}(f)}{(2K_D P_0)^2} = -130 \text{ dB/Hz}, \tag{10a}$$

$$S_{\delta P}(f) = 3.9 \times 10^{-23} \text{ W}^2/\text{Hz}, \tag{10b}$$

which is equivalent to a NEP of $6 \text{ pW}/\sqrt{\text{Hz}}$. These last figures give only a rough estimation of the diode ability to detect small power variations. Indeed they do not report the detector intrinsic noise $S_{i_d}(f)$ and especially its possible flicker (or $1/f$) component.

IV. DIODE CHARACTERISTICS MEASUREMENTS

Two identical DT8012 diodes have been tested. The microwave signal is distributed to these diodes by a Wilkinson power divider. This assembly is fastened to the 2nd stage of a pulse-tube cryocooler (model CryoMech PT-403). Three low thermal conductivity coaxial semi-rigid cables connect this set to feedthroughs placed on the cryostat top flange. Once the room temperature measurements are realized, the cryocooler is turning on. The 2nd stage temperature stabilizes at 4 K in less than 20 h. No temperature control has been implemented. However during the measurement the mean temperature is stable within $\pm 0.2 \text{ K}$.

A. Power-to-voltage gain

The measurement of K_D is straightforward. The video amplifier output voltage V_{out} is recorded as a function of the input RF power. The result is eventually divided by the dc-gain of the video amplifier. The characteristics recorded at room temperature and 4 K are given in Fig. 3.

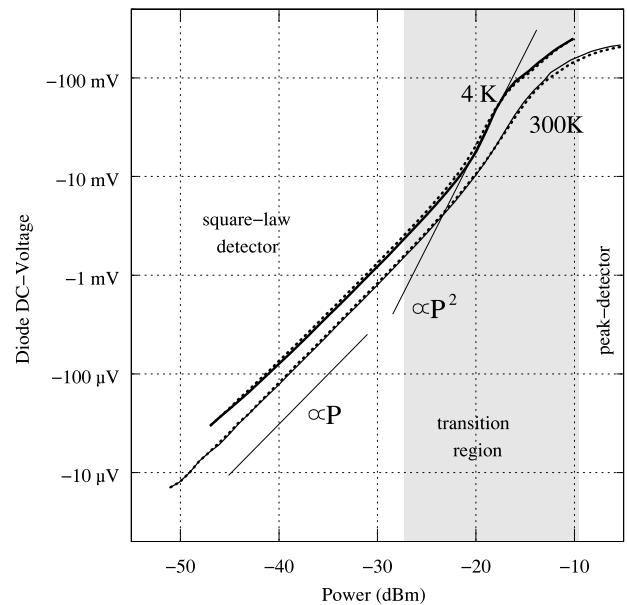


FIG. 3. Power-to-Voltage gain of the tunnel diodes measured at room temperature and 4 K. The signal frequency is $\nu_0 = 10 \text{ GHz}$, and the amplifier input resistance is $R_L = 1 \text{ M}\Omega$. Solid line: SN436409. Dotted line: SN436410.

We can distinguish three different types of operation. At very low input power, i.e., $P_0 \leq -30 \text{ dBm}$, the diode behaves like a perfect square-law detector. Its output dc-voltage is proportional to the input power as expected. The sensitivity $K_D \approx 850 \text{ V/W}$ at room temperature and increases up to 1200 V/W at 4 K. At high input power, the diode acts like a peak detector. In between, the voltage-to-power slope indicates that the output voltage depends on the square of the incoming signal power. It is obvious that Equation (5) is no valid in this region and its application can induce serious inaccuracy in power measurements. The same behavior has been observed in room temperature Schottky diode detectors.¹³ In this case it has been demonstrated that this behavior is inherent to the diode exponential current-voltage characteristic. The tunnel diode characteristic does not follow the Schottky diode equation but an exponential form can be derived as well.^{14,15} In our applications the RF signal power is often in the transition region, and thus we need to clarify the detector sensitivity.

B. Differential gain

We define the first-derivative of the function $\kappa_D(P)$ evaluated at $P = P_0$ as the differential gain of the diode. It can be easily measured by using the set-up depicted in Fig. 4.

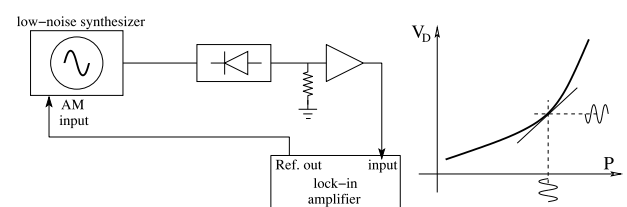


FIG. 4. Differential gain measurement. The synthesizer is a Keysight E-8257D, and the lock-in amplifier is a Stanford Research SR810.

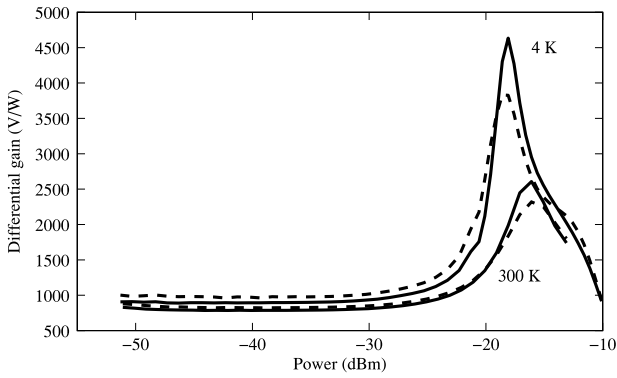


FIG. 5. Tunnel diode differential gain measured at room temperature and 4 K. The signal frequency is $\nu_0 = 10$ GHz, and the amplifier input resistance is $R_L = 1$ M Ω . The modulation frequency was 70 kHz, and the modulation index was 2×10^{-2} . Solid lines: SN436409. Dashed lines: SN436410.

We intentionally modulate the signal amplitude with a known small deviation and detect with a lockin amplifier the resulting ac-voltage at the detector output. The measured differential gain as a function of incoming power is represented in Fig. 5.

At a very low power the differential gain is almost constant and compatible with the previous measurements. However it shows a dramatic increase in the transition region corresponding to the change in the slope in Figure 3. At 4 K and around -17 dBm the diode is approximately four times as sensitive as at low power. Then above approximately -13 dBm the differential gain rapidly drops. The change in sensitivity is less abrupt at room temperature but still exists. This change should be absolutely taken into account in the following to determine with accuracy the noise floor of the AM detection.

The non-linear behavior of the detector is also attested by the presence of harmonics of the AM frequency at the diode output. These harmonics come from the higher order terms in the development of $\kappa_D(P)$ neglected in Equation (6). Figure 6 gives the level of harmonics for a AM frequency of 3 kHz and a modulation index of 0.2.

To facilitate a fast and sensitive measurement of the high order harmonics, we deliberately decreased the frequency and increased the index of the modulation. For a modulation index of 10^{-2} , we only checked that the second harmonic shows the same behavior observed in Fig. 6.

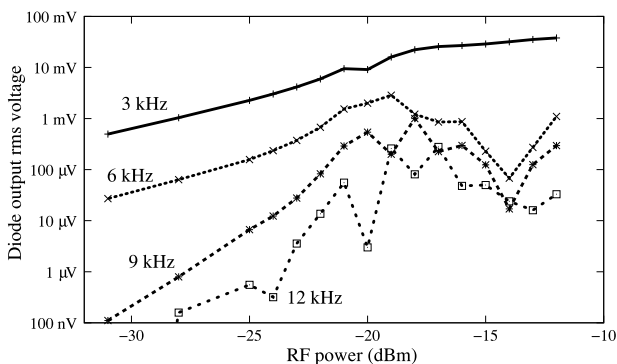


FIG. 6. Harmonics in the diode output voltage. The RF signal frequency is $\nu_0 = 10$ GHz, and the amplifier input resistance is $R_L = 1$ M Ω . The AM frequency was 3 kHz, and the modulation index was 2×10^{-1} . Diode SN436409.

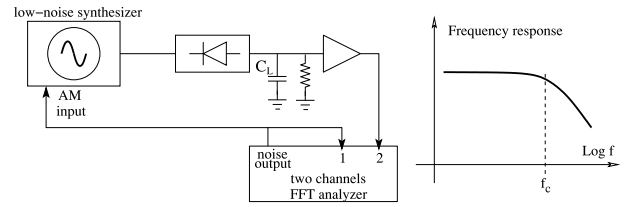


FIG. 7. Video bandwidth measurement. The added capacitance is $C_L = 100$ nF. The synthesizer is a Keysight E-8257D.

C. Differential resistance

The diode differential resistance R_D appears in the detector noise budget given by the Equation (9). We determine its variation as a function of the RF signal power with the set-up schematized in Figure 7.

In the simplest configuration depicted in Figure 1, the video bandwidth is larger than 100 kHz. Indeed the high load resistance ($R_L = 1$ M Ω) is shorted by the diode differential resistance: $R_L \gg R_D$. By adding a large capacitance $C_L = 100$ nF, the cutoff frequency $f_C \approx (2\pi R_D C_L)^{-1}$ is shifted below 100 kHz. f_C can be easily measured with a baseband fast Fourier transform analyzer. Fig. 8 shows R_D as a function of the signal power. We note that the transition region is characterized by an strong increase of R_D .

V. NOISE MEASUREMENT

A detector alone can be measured only if a reference source is available whose AM noise is lower than the detector noise and if the amplifier noise can be made negligible. These are unrealistic requirements. A more sophisticated approach is to compare two detectors, A and B as shown in Figure 9.

The first arm (bold line) takes the differential signal $g(P_b - P_a) \approx 0$, which is not affected by the power fluctuation of the source. The voltage PSD measured at the output still contains the contribution of the video amplifiers' noise sources. Thus a second arm identical to the first one measures also $g(P_b - P_a)$. By measuring the cross spectrum at the output of two arms we eliminate the contribution of the intrinsic voltage noise source e_n of each video amplifier. The noise current i_n of the video-amplifier turns into correlated random

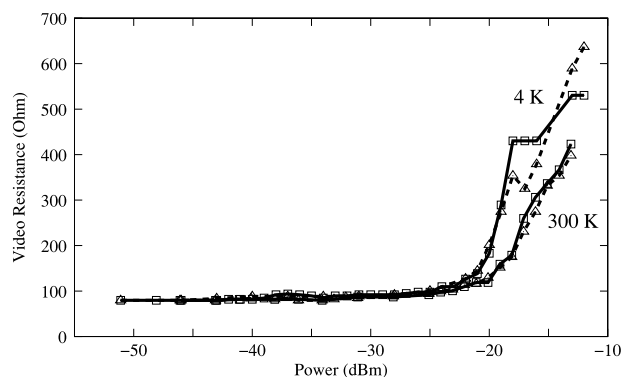


FIG. 8. Diode differential resistance R_D as determined from the measurement of the video bandwidth in presence of the additional capacitor $C_L = 100$ nF. Solid lines: SN436409. Dashed lines: SN436410.

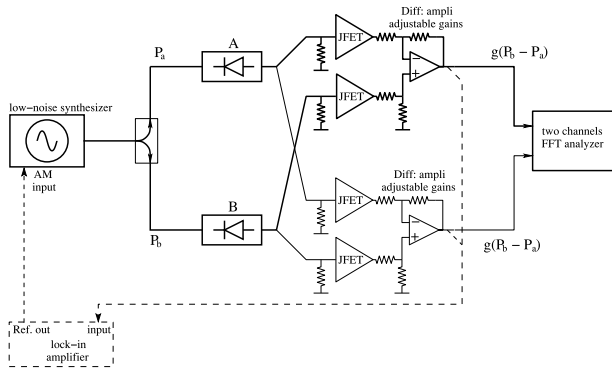


FIG. 9. Two-channel correlation measurement set-up. The lockin amplifier is used to adjust the gains of the differential amplifiers.

voltage fluctuations across each diode video resistance and thus is not eliminated by correlation. Using a JFET operational amplifier makes the current noise contribution negligible. Figure 10 shows the typical diode voltage PSD obtained with the two diodes at 4 K and receiving -20 dBm. We assume that the two detectors are equivalent: 3 dB has been subtracted from the measured spectrum.

The video-amplifier voltage noise e_n has been measured with a 50Ω input load (dashed line): $e_n = 5 \text{ nV}/\sqrt{\text{Hz}}$. On each channel this noise floor masks the diode intrinsic noise for Fourier frequencies higher than 1 kHz. The latter is revealed by the cross-spectrum (bold line). The diode noise is dominated by a flicker ($1/f$ slope) component and a white noise floor reaching approximately $-173 \text{ dB V}^2/\text{Hz}$ for $f > 30 \text{ kHz}$.

It is useful to express the intrinsic diode noise in terms of $S_{\delta P}(f)$ (power fluctuation PSD) or $S_{\alpha}(f)$ (relative amplitude fluctuation PSD). Combining Equations (4) and (6), they are related to the experimental measurement of diode voltage PSD as

$$S_{\delta P}(f) = \left[\frac{1}{\kappa'_D(P_0)} \right]^2 S_{\delta V_d}(f), \quad (11a)$$

$$S_{\alpha}(f) = \left[\frac{1}{2P_0\kappa'_D(P_0)} \right]^2 S_{\delta V_d}(f), \quad (11b)$$

where $\kappa'_D(P_0)$ is the diode differential gain measured at P_0 . $S_{\alpha}(f)$ is presented in Fig. 11.

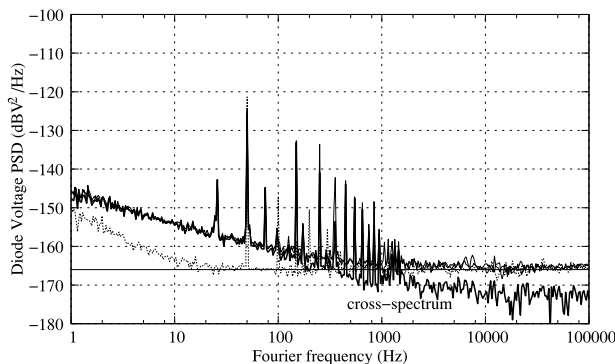


FIG. 10. Diode voltage PSD at 4 K and -20 dBm signal power. Thin lines: PSD of each channel. Bold line: cross-spectrum. Dashed line: single channel noise floor.

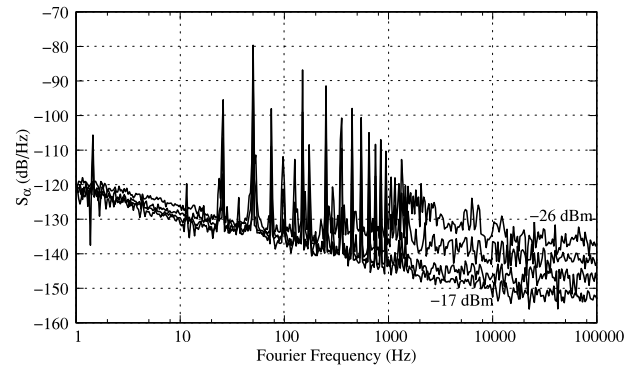


FIG. 11. Diode intrinsic noise expressed as the relative amplitude fluctuation PSD of the incoming RF signal. $S_{\alpha}(f)$ is measured at 4 K for -26 , -23 , -20 , and -17 dBm input signal powers.

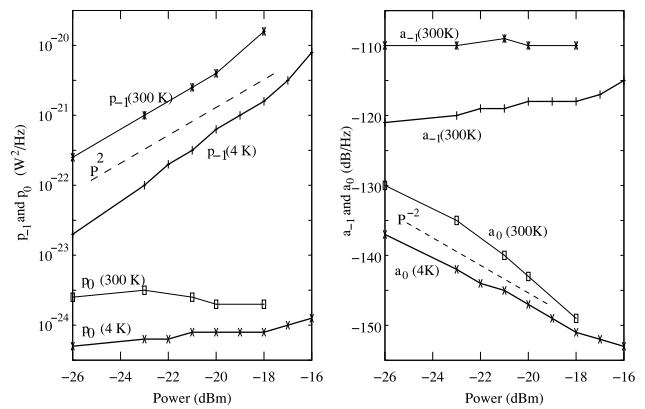


FIG. 12. White and flicker noise components for $S_{\delta P}$ and S_{α} measured at 4 K and 300 K.

To keep the figure readable, we only present the PSDs for four signal powers. The same measurements have been done at room temperature. All the recorded cross-spectrum shows a white noise floor and flicker component, and we approximate the two PSDs as

$$S_{\delta P}(f) = \frac{p_{-1}}{f} + p_0 \quad \text{and} \quad S_{\alpha}(f) = \frac{a_{-1}}{f} + a_0. \quad (12)$$

Figure 12 gives the coefficients p_{-1} , p_0 , a_{-1} , and a_0 as a function of the signal power at 4 K and 300 K.

In terms of power fluctuation PSD, the white noise floor is independent of the signal power. For $f > 10 \text{ kHz}$, $S_{\delta P} = 6.3 \times 10^{-25} \text{ W}^2/\text{Hz}$, equivalent to a NEP of $0.8 \text{ pW}/\sqrt{\text{Hz}}$. The flicker noise increases proportionally to P^2 . The same dependency has been reported in Ref. 19. When expressed as S_{α} , the flicker noise appears independent of the incoming power. The relative amplitude fluctuation PSD is about -120 dB/Hz at 1 Hz. The room temperature measurements are about 10 dB higher.

VI. CONCLUSION

We characterized commercial tunnel diode low-level microwave power detectors intended to be implemented in a cryogenic sapphire oscillator. At 4 K, these diodes can only be considered as nearly perfect square-law detectors for

incident microwave power below -30 dBm. Around -20 dBm, the diode differential gain presents a dramatic increase. This strong non-linearity contradicts the generally admitted model of a square-law detector smoothly saturating with the incident signal power.

A high sensitivity two-channel correlation measurement set-up has been used to measure the noise of the diode detector as a function of the incident power. It is shown that $S_{\alpha}(f)$, the PSD of fractional amplitude fluctuations, presents a flicker noise component almost independent of the incoming power. At 4 K, $S_{\alpha}(f) \approx 10^{-12}/f$. In the presence of such a flicker noise, the fractional amplitude stability expressed in terms of Allan deviation²⁰ will be 1.2×10^{-6} . For a room temperature diode the limit is 3.7×10^{-6} .

ACKNOWLEDGMENTS

The work has been realized in the frame of the ANR projects: EquipEX Oscillator-Imp and LabEX First-TF. The authors would like to thank the Council of the Région de Franche-Comté for its support to the Projets d'Investissements d'Avenir.

¹C. Burrus, "Backward diodes for low-level millimeter-wave detection," *IEEE Trans. Microwave Theory Tech.* **11**(5), 357–362 (1963).

²A. Cowley and H. Sorensen, "Quantitative comparison of solid-state microwave detectors," *IEEE Trans. Microwave Theory Tech.* **14**(12), 588–602 (1966).

³W. F. Gabriel, "Tunnel-diode low-level detection," *IEEE Trans. Microwave Theory Tech.* **15**(10), 538–553 (1967).

⁴S. Grop, P. Y. Bourgeois, N. Bazin, Y. Kersalé, E. Rubiola, C. Langham, M. Oxborrow, D. Clapton, S. Walker, J. De Vicente, and V. Giordano, "ELISA: A cryocooled 10 GHz oscillator with 10^{-15} frequency stability," *Rev. Sci. Instrum.* **81**(2), 025102 (2010).

⁵V. Giordano, S. Grop, B. Dubois, P.-Y. Bourgeois, Y. Kersalé, E. Rubiola, G. Haye, V. Dolgovskiy, N. Bucalovicy, G. D. Domenico, S. Schilt, J. Chauvin, and D. Valat, "New generation of cryogenic sapphire microwave oscillator for space, metrology and scientific applications," *Rev. Sci. Instrum.* **83**(8), 085113 (2012).

⁶C. Fluhr, S. Grop, B. Dubois, Y. Kersalé, E. Rubiola, and V. Giordano, "Characterization of the individual frequency stability of Cryogenic Sapphire Oscillators at the 10^{-16} level," *IEEE Trans. Ultrason., Ferroelectr. Freq. Control* **6**, 915–921 (2016).

⁷Z. Galani, M. Bianchini, R. Waterman, R. Dibiase, R. Laton, and J. Cole, "Analysis and design of a single-resonator GaAs FET oscillator with noise degeneration," *IEEE Trans. Microwave Theory Tech.* **32**(12), 1556–1565 (1984).

⁸R. Pound, "Electronic frequency stabilization of microwave oscillators," *Rev. Sci. Instrum.* **17**(11), 490–505 (1946).

⁹V. Giordano, S. Grop, P. Y. Bourgeois, Y. Kersalé, and E. Rubiola, "Influence of the electron spin resonance saturation on the power sensitivity of cryogenic sapphire resonators," *J. Appl. Phys.* **116**(5), 054901 (2014).

¹⁰N. R. Nand, S. R. Parker, E. N. Ivanov, J. M. Le Floch, J. G. Hartnett, and M. E. Tobar, "Resonator power to frequency conversion in a cryogenic sapphire oscillator," *Appl. Phys. Lett.* **103**, 043502 (2013).

¹¹C. R. Locke, E. N. Ivanov, J. G. Hartnett, P. L. Stanwix, and M. E. Tobar, "Invited Article: Design techniques and noise properties of ultrastable cryogenically cooled sapphire-dielectric resonator oscillators," *Rev. Sci. Instrum.* **79**(5), 051301 (2008).

¹²H. Rothe and W. Dahlke, "Theory of noisy fourpoles," *Proc. IRE* **44**(6), 811–818 (1956).

¹³R. G. Harrison and X. Le Polozec, "Nonsquarelaw behavior of diode detectors analyzed by the Ritz-Galerkin method," *IEEE Trans. Microwave Theory Tech.* **42**(5), 840–846 (1994).

¹⁴T. A. Demassa and D. P. Knott, "The prediction of tunnel diode voltage-current characteristics," *Solid State Electron.* **13**(2), 131–138 (1970).

¹⁵P. J. De Maagt, T. F. Buss, V. Roer, and T. G. De, "Temperature dependence of Schottky versus backward diodes for radiometry applications," *Micro-wave Opt. Technol. Lett.* **5**(7), 295–299 (1992).

¹⁶C. A. Hoer, K. C. Roe, and C. M. Allred, "Measuring and minimizing diode detector nonlinearity," *IEEE Trans. Instrum. Meas.* **1001**(4), 324–329 (1976).

¹⁷V. S. Reinhardt, C. Shih, P. Toth, S. C. Reynolds, A. L. Berman *et al.*, "Methods for measuring the power linearity of microwave detectors for radiometric applications," *IEEE Trans. Microwave Theory Tech.* **43**(4), 715–720 (1995).

¹⁸D. K. Walker, K. J. Coakley, and J. D. Splett, "Nonlinear modeling of tunnel diode detectors," in *Proceedings of the 2004 IEEE International Geoscience and Remote Sensing Symposium, IGARSS'04* (IEEE, 2004), Vol. 6, pp. 3969–3972.

¹⁹S. T. Eng, "Low-noise properties of microwave backward diodes," *IRE Trans. Microwave Theory Tech.* **9**(5), 419–425 (1961).

²⁰E. Rubiola, *Phase Noise and Frequency Stability in Oscillators* (Cambridge University Press, 2008), ISBN: 978-0-521-88677-2.